

PETROGRAPHIC, FLUID INCLUSION AND OXYGEN ISOTOPE CHARACTERISTICS OF RAMAND AREA, NW IRAN

PETROGRAFIA, FLUIDO DE INCLUSÃO E ISÓTOPO DE OXIGÊNIO CARACTERÍSTICOS DA ÁREA DE RAMAND, NW DO IRÃ

PETROGRAFÍA, LÍQUIDO DE INCLUSIÓN Y CARACTERÍSTICAS DEL ISÓTOPO DE OXÍGENO DEL ÁREA DE RAMAND, NW DE IRÁN

<https://doi.org/10.26895/geosaberes.v11i0.1047>

SIMA BOOTORABI ¹
REZA MEHRNIA ^{2*}
AHMAD KHAKZAD ³
NIMA NEZAFATI ⁴

¹ PhD Student, Department of Geology, Faculty of Basic Sciences, Islamic Azad University, Science and Research Branch, Tehran, Iran. CP:4917746846, Tel.: (+98) 9127863178, bootorabi44@gmail.com, <http://orcid.org/0000-0002-2604-7304>

² Department of Geology, Payam-e Noor University, Iran. CP: 1959915584, Tel.: (+98) 9122574607, srmehrnia@yahoo.com, <http://orcid.org/0000-0001-9801-4707>

* Corresponding author

³ Professor, Department of Geology, Faculty of Basic Sciences, Islamic Azad University, North Tehran Branch, Tehran, Iran. CP: 4917746846, Tel.: (+98) 9121027553, profahmadkhakzad@yahoo.com, <http://orcid.org/0000-0001-5665-1935>

⁴ Assistant Professor, Department of Geology, Faculty of Basic Sciences, Islamic Azad University, Science and Research Branch, Tehran, Iran. CP: 1738633467, Tel.: (+98) 09128083577, nima.nezafati@gmail.com, <http://orcid.org/0000-0002-5806-343X>

Article History:

Received on 14 from January of 2020.

Accepted on 25 of February of 2020.

Published in 04 of July of 2020.

ABSTRACT

Ramand mineralization area is located at a distance of about 60 km from the provincial capital of Qazvin province, Iran. The studied area is a part of the Central Iran structural zone in the southern part of Danesfahan geological map. Lithological units in Ramand area are composed of riodacite, rhyolite, tuff riodacite, crystal tuff and riodacite. The presence of clay minerals indicates argillic alteration, which is a good indicator of mineralization. This type of alteration can be detected in volcanic regions which have been severely affected by argillic alteration. Silicification is the most important evidence of precious metal potential in post magmatic environments. According to mineralogical studies, sulfide minerals in the area consist of pyrite and chalcopyrite with supergene minerals such as covellite, malachite, and Fe hydroxides. Based on phase content, the three types of inclusion in Ramand area include vapor, vapor liquid, and liquid rich inclusions. According to fluid inclusion data, the liquid vapor homogenization temperature [$T_{H(L-V)}$] varied from 73 to 307 °C, and salinity ranged from 1.75 to 4.74 wt% NaCl eq. The calculated $\delta^{18}O$ values of water in equilibrium with quartz ranged from 5.8 to 6.9 per ml. Calculated $\delta^{18}O$ values of water in equilibrium with calcite ranged from 4.4 to 9.4 per ml. These data suggest that the ores formed most likely originated from magmatic hydrothermal sources along with some meteoric solutions during mineralization processes.

Keywords: Qazvin. Fluid inclusion. Oxygen isotopic. Petrography. Mineralization.

RESUMO

A área de mineralização de Ramand está localizada a uma distância de cerca de 60 km da capital da província de Qazvin, no Irã. A área estudada faz parte da zona estrutural do Irã Central, na parte sul do mapa geológico de Danesfahan. As unidades litológicas na área de Ramand são compostas por riodacito, riolito, tufo de riodacito, tufo de cristal e riodacito. A presença de minerais argilosos indica alteração argílica, que é um bom indicador de mineralização. Este tipo de alteração pode ser

Geosaberes, Fortaleza, v. 11, p. 450-466, 2020.

Copyright © 2010, Universidade Federal do Ceará

detectado em regiões vulcânicas que foram severamente afetadas pela alteração argílica. A silicificação é a evidência mais importante do potencial de metais preciosos em ambientes pós-magmáticos. De acordo com estudos mineralógicos, os minerais sulfetados na área consistem em pirita e calcopirita com minerais supergênicos, como covellite, malaquita e hidróxidos de Fe. Com base no conteúdo da fase, os três tipos de inclusão na área de Ramand incluem inclusões de vapor, vapor líquido e líquido rico. De acordo com os dados de inclusão de fluidos, a temperatura de homogeneização do vapor líquido [$T_{H(L-V)}$] variou de 73 a 307 ° C, e a salinidade variou de 1,75 a 4,74% em peso de NaCl eq. Os valores calculados de $\delta^{18}O$ da água em equilíbrio com o quartzo variaram de 5,8 a 6,9 por ml. Os valores calculados de $\delta^{18}O$ da água em equilíbrio com calcita variaram de 4,4 a 9,4 por ml. Esses dados sugerem que os minérios formados provavelmente se originaram de fontes hidrotérmicas magmáticas, juntamente com algumas soluções meteóricas durante os processos de mineralização.

Keywords: Qazvin. Inclusão fluida. Isotópico de oxigênio. Petrografia. Mineralização.

RESUMEN

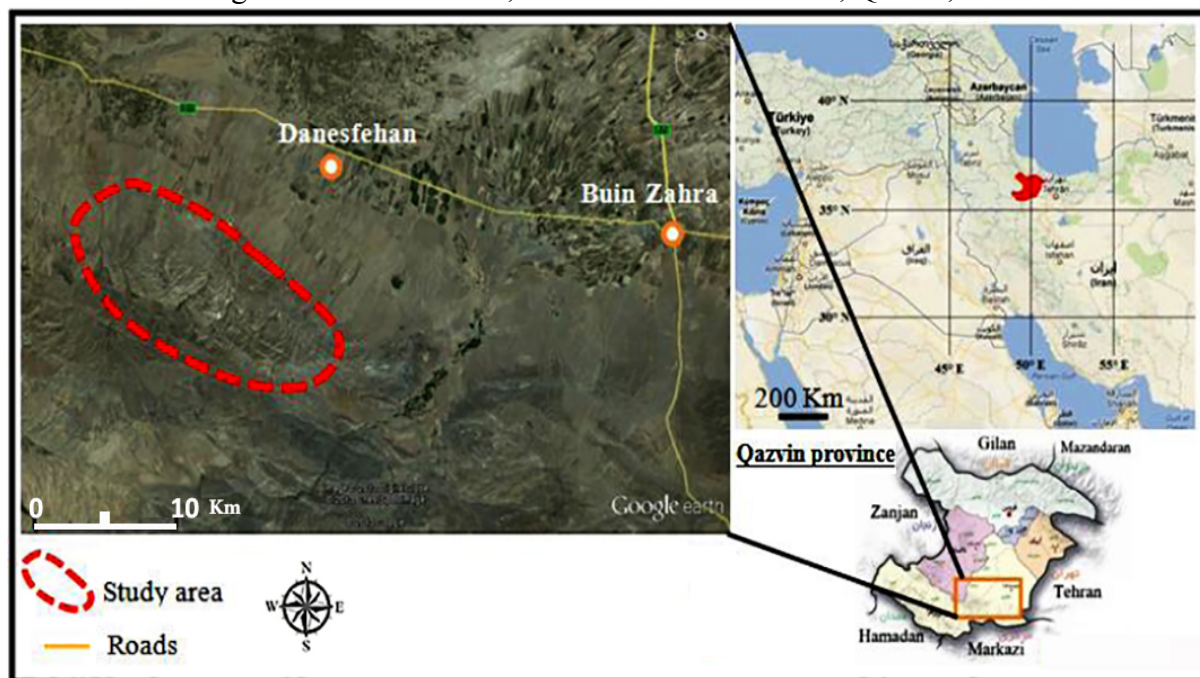
El área de mineralización de Ramand se encuentra a una distancia de unos 60 km de la capital provincial de la provincia de Qazvin, Irán. El área estudiada es parte de la zona estructural del centro de Irán en la parte sur del mapa geológico de Danesfahan. Las unidades litológicas en el área de Ramand se componen de riodacita, riolita, toba riodacita, toba de cristal y riodacita. La presencia de minerales arcillosos indica alteración argílica, que es un buen indicador de mineralización. Este tipo de alteración puede detectarse en regiones volcánicas que han sido severamente afectadas por la alteración argílica. La silicificación es la evidencia más importante del potencial de metales preciosos en entornos post magmáticos. De acuerdo con estudios mineralógicos, los minerales de sulfuro en el área consisten en pirita y calcopirita con minerales supergênicos tales como la calallita, la malaquita y los hidróxidos de Fe. Según el contenido de fase, los tres tipos de inclusión en el área de Ramand incluyen vapor, vapor líquido e inclusiones ricas en líquido. Según los datos de inclusión de líquidos, la temperatura de homogeneización del vapor líquido [$T_{H(L-V)}$] varió de 73 a 307 ° C, y la salinidad varió de 1.75 a 4.74% en peso de NaCl eq. Los valores calculados de $\delta^{18}O$ del agua en equilibrio con cuarzo oscilaron entre 5,8 y 6,9 por ml. Los valores calculados de $\delta^{18}O$ del agua en equilibrio con calcita oscilaron entre 4,4 y 9,4 por ml. Estos datos sugieren que los minerales formados probablemente se originaron de fuentes hidrotermales magmáticas junto con algunas soluciones meteóricas durante los procesos de mineralización.

Keywords: Qazvin. Inclusión de fluidos. Oxígeno isotópico. Petrografía. Mineralización.

INTRODUCTION

The petrographic study of a rock sample is the first essential step in any fluid inclusion study. Most copper deposits, especially those formed by hydrothermal activities, have been formed by magmatism in the Tertiary to Quaternary interval and are discovered in continental and oceanic arcs (COOKE et al., 2005). These deposits show similar vein patterns and distribution of alteration (GUSTAFSON & HUNT, 1975; BEANE & BODNAR, 1995; SEEDORF, 2005). Copper deposits in Iran, such as those occurring in the Urumieh-Dokhtar magmatic belt, have been formed due to subduction of the Arabian Plate beneath Central Iran micro-continent during the Cenozoic Alpine orogeny (NIAZI et al., 1978; BERBERIAN, 1981; BERBERIAN & KING, 1981). The ore deposits are often produced by fluid flow processes which alter mineralogy and chemistry of rocks. Previous literature confirms the reliability of multispectral data analysis in the field of alteration detection. Most zonally distributed ore deposits are first detected in the field by recognition of hydrothermally-altered host rocks. Economic mineralization often occurs by fluid processes that substantially alter the mineralogy and chemistry of the host rocks. This alteration is capable of producing distinctive assemblages of minerals that vary according to the location, degree and longevity of those flow processes. When exposed on the surface of the Earth, this alteration can sometimes be mapped as a zonal pattern. Ramand region in the northwest of Iran (Figure 1) is an important area due to the good mineralization of copper, lead, zinc and precious metals such as gold and silver. The results presented in this paper have implications for the genetic models of copper and auriferous quartz vein systems in Ramand region.

Figure 1 - Ramand area, southwest of Buin Zahra, Qazvin, Iran



GEOLOGICAL SETTING

According to the depositional-structural division of Iran (AGHANABATI, 2004), Ramand area is located in the northwestern margin of Central Iran. Tectonically, it is located in Orumiyeh-Dokhtar zone (BAZARGANI-GUILANI et al., 2008). The Hasanabad fault is the major fault passing through the study area and Ramand Mountain is located on its northern side. One of the old faults in the study area, Hasanabad fault is considered the dominant active fault in Ramand region. This fault has been influenced by new movements and has been active during the Quaternary. The Buin Zahra earthquake, with a magnitude of larger than 7.25 on the Richter scale, occurred along this fault and devastated the adjacent villages, confirming the recent activity of the fault. Hasanabad fault is the continuation of Buin Zahra fault with dominant compressional movements, southward dip and strike-slip inclinations. Furthermore, a larger number of faults with a northwest-southeast dominant trend are present in the study area (EZZATI et al., 2014). Ramand Mountain is located in the northwestern corner of Saveh 1:250,000 geological map and the central part of Danesfehan map (Khiaraj 1:100,000) (Figure 2). The host rock units of the alteration are mainly composed of rhyodacitic-rhyolitic igneous rocks and tuff (Figure 3). Based on the field investigations and the results of XRD analyses, acidic and intermediate volcanic rocks of Ramand Mountain have variably undergone hydrothermal alteration, sometimes in dispersed form under the influence of ascending hydrothermal fluids. The extensive alterations in the study area mostly include argillic and silica phase alterations. Silicified formations are the most common alteration in the hydrothermal system. Silicified formations are exposed in some parts of the wall rock as silicification and in some part in the form of jasperoid (Figure 4). Geochemical and petrographical characteristics of acidic volcanic rocks in the south of Danesfehan reflect the role of different petrogenesis processes in the formation of these types of rocks (Figure 5). Magmatic differentiation through fractional crystallization is the main process involved in the formation of most of these rocks in the study area (MANSOURI, 1998; MEHRNIA, 2015).

Figure 2 - Geological map of Ramand region in the Qazvin province

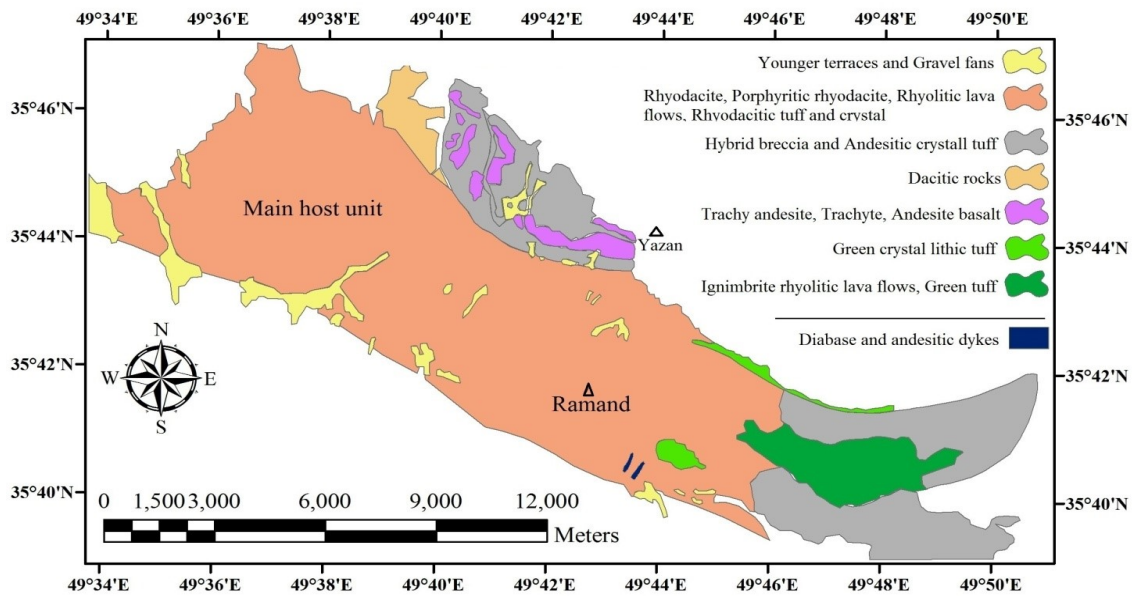


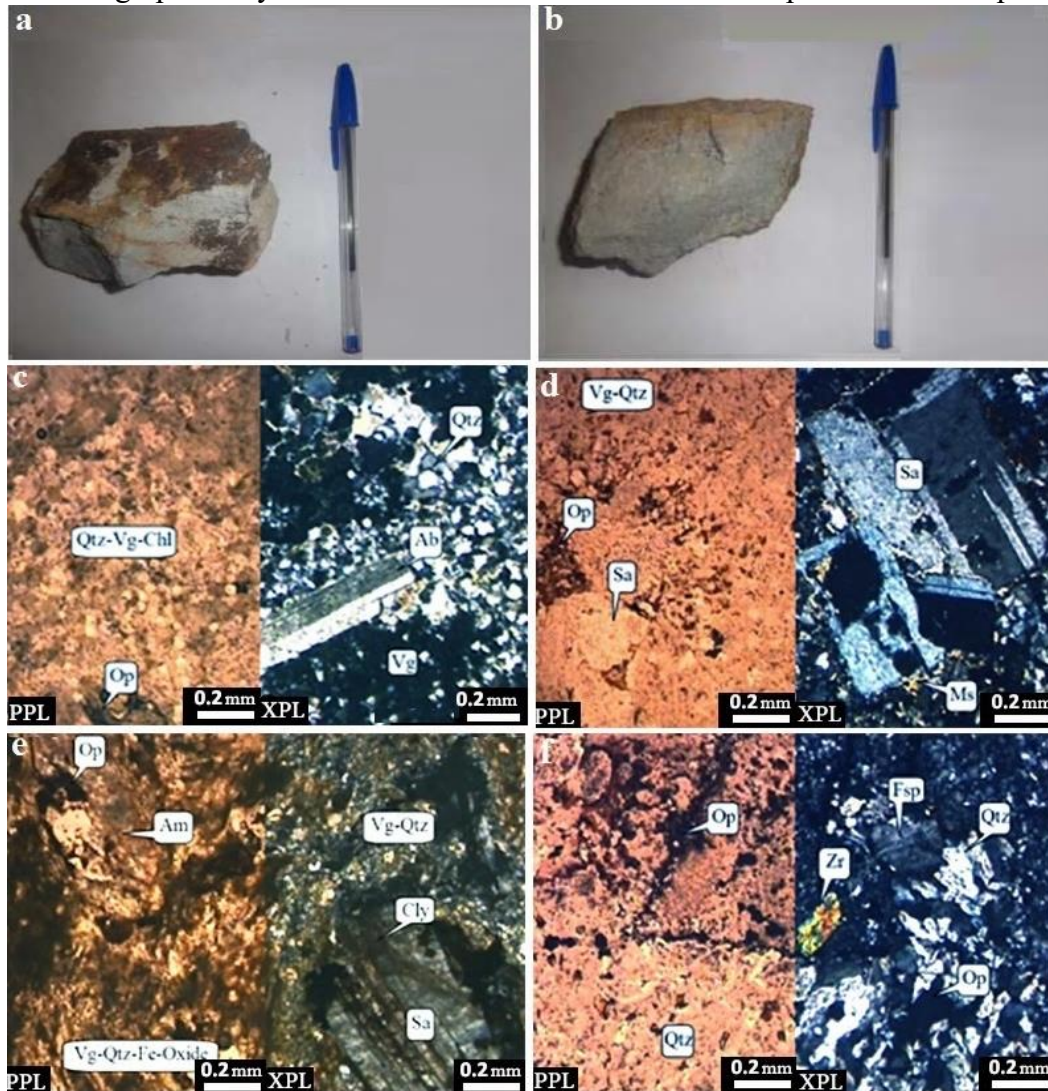
Figure 3 - Fe-bearing Silica minerals in study area (see to the southwest), a) Brecciated volcanic rocks, b) Si, Fe oxide alteration



Figure 4 - The higher values of iron oxides have led to a red matrix (probably due to the presence of jasperoid) (Py: Pyrite, scale: 2 mm)



Figure 5 - Photomicrographs of host rock and ores from the Ramand area. **a)** photograph showing rhyolite as host rock, **b)** photographs of rhyodacite, **(c, d)** photomicrograph showing the volcanic host rock; the grains are mainly quartz and feldspar (Sanidine, Albite) and **(e, f)** photomicrograph of rhyolite. Smaller amounts of zircon and amphibole are also present.



MATERIALS AND METHODS

A number of samples were collected from the mineral veins, ores and gangue of different paragenetic phases and outcrops at the Ramand mineral indices. A total of 7 thin sections, 6 polished thin sections and 4 doubly-polished thin sections were prepared for petrographic and fluid inclusion studies. A total of 13 polished thin sections were examined under transmitted and reflected light at Iranian Mineral Processing Research Center (IMPRC). Micro-thermometric studies were carried out on doubly-polished thin sections. Phase change temperatures in fluid inclusions were measured using a Fluid Inc. Linkam-type gas-flow stage at IMPRC laboratory by passing precooled N₂ gas around the sample. Stage calibration was performed using synthetic fluid inclusions. The standard reference temperatures were measured with an accuracy of $\pm 0.2^{\circ}\text{C}$ at -94.3°C (triple point of CO₂). An approximate heating rate of $\pm 0.6^{\circ}\text{C}/\text{min}$ was used near the phase transition temperatures. Oxygen isotope analyses were performed on 6 pure quartz and calcite crystals collected from the

mineralized veins. Isotope ratios were measured on a Finnigan–MAT 252 multi-collector mass spectrometer at AcmeLabs, Canada.

RESULTS

Hydrothermal Alteration and Mineralization

Hydrothermal alteration and mineralization in Ramand area are centered on the rhyolitic igneous rocks. Based on petrography and mineralogy of the collected samples, silicic, phyllic, argillic and propylitic alterations were found in the Ramand area. The early hydrothermal alteration was predominantly of silicic and argillic nature followed by phyllic and propylitic alterations. In general, silicic alteration has a relatively large extension but propylitic alteration has a limited distribution in the Ramand area. Furthermore, the highest copper grade was observed in the silicic alteration. Argillic alterations consist of clay minerals such as kaolinite, montmorillonite, illite, pyrophyllite as well as goethite, jarosite, hematite, sericite, chlorite and quartz. Clay minerals have been produced from alteration of K-feldspar. The affected rocks are soft and white, but can change to a brown color with the increasing iron-oxide content. Phyllic alteration is caused by leaching of sodium, calcium and magnesium from aluminosilicate-bearing rocks. During this alteration, almost all rock-forming silicates are replaced by sericite and quartz. Propylitic alterations consists of calcite, chlorite, epidote, sericite, actinolite, and pyrite. Propylitic alteration is represented by chloritization of primary and secondary biotite and epidotization of plagioclase. Plagioclase is locally replaced by clays and sericite. Also, amphibole phenocrysts are partly altered to chlorite. Ore microscopy and petrographic studies were conducted on polished thin sections to examine mineralogical peculiarities of the samples (Figures 6, 7). The two micrographs in Figure 8 show paragenesis of available ore minerals (Fig. 8b) with nonmetallic aggregations as gangue traces (Figure 8a). Pyrite and hematite are well-known forms of mineralization at the surface of remotely-sensed alterations (Fig. 8b). According to petrographic evidence (Figure 8a), a massive silicified texture (fine-grained) has also been intruded by quartz and Fe-hydroxides. From a mineralogical point of view, a massive silica facies in paragenetic association with Fe-oxide and Fe-sulfide minerals has enough potential for increasing gold-trace anomalies. Therefore, atomic absorption analysis (AA) was also carried out and the results analysis for gold are listed in Table 1. As is clearly seen, Au-grade varies from 131 to 145 ppb in the vicinity of alterations which mostly contain argillic-silicific sequences. Individual shiny pyrite crystals with a bright appearance are more reflective (compared with pale types) and were therefore selected for detailed quantitative analysis by scanning electron microscopy (SEM). Mineralogical analytical evidence and SEM micrographs indicate that Ramand altered region has potential for base metals and gold prospecting (Figure 9). An increase in silica content is directly related to pyrite and invisible gold traces associated with quartz-agate veinlets in post-magmatic differential stages of hydrothermal environments.

Figure 6 - **a)** Subhedral chalcopyrite crystal in goethite matrix (covellite replaces chalcopyrite), **b)** euhedral and subhedral chalcopyrite crystal, **c)** photograph of Cu mineralization in silica veins, likely chalcopyrite, **d)** magnetite is converted into hematite, **e)** covellite replacing chalcopyrite (plain-polarized reflected light), **f)** malachite filling the cracks in goethite. (Abbreviations: Py: pyrite, Ccp: chalcopyrite, Hem: hematite, Mag: magnetite, Mal: malachite, Gt: goethite, Cv: covellite, Mu: muscovite, Au: Gold, Gan: gangue).

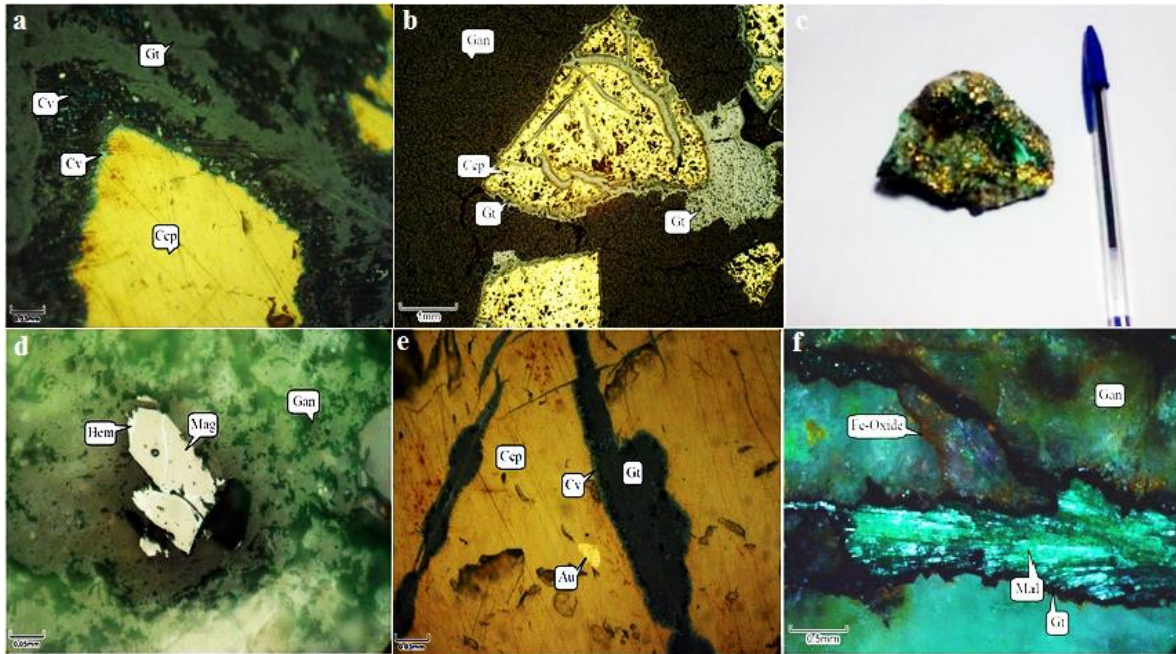


Figure 7 - Photomicrographs of ores from the Ramand area: **a)** Subhedral pyrite crystal in Fe-oxide matrix, and **(b, c, d)** pyrite replacing magnetite and hematite

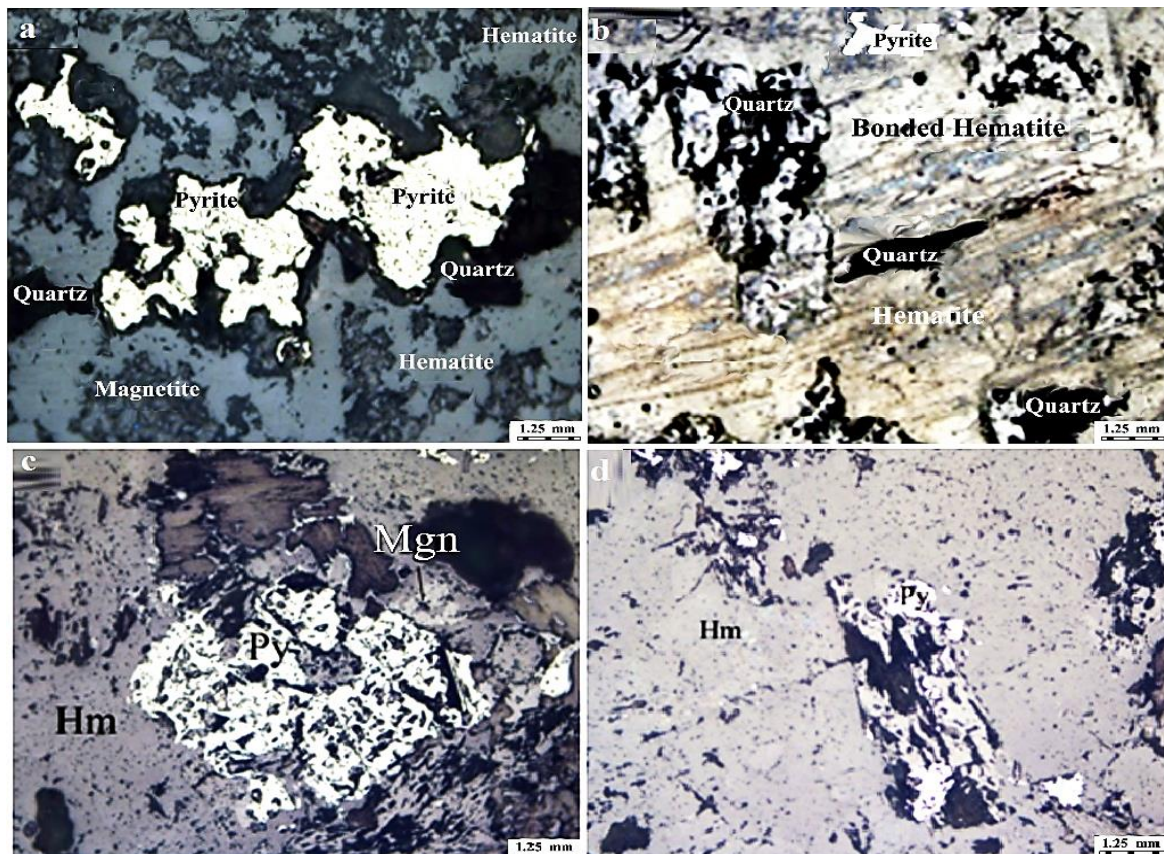
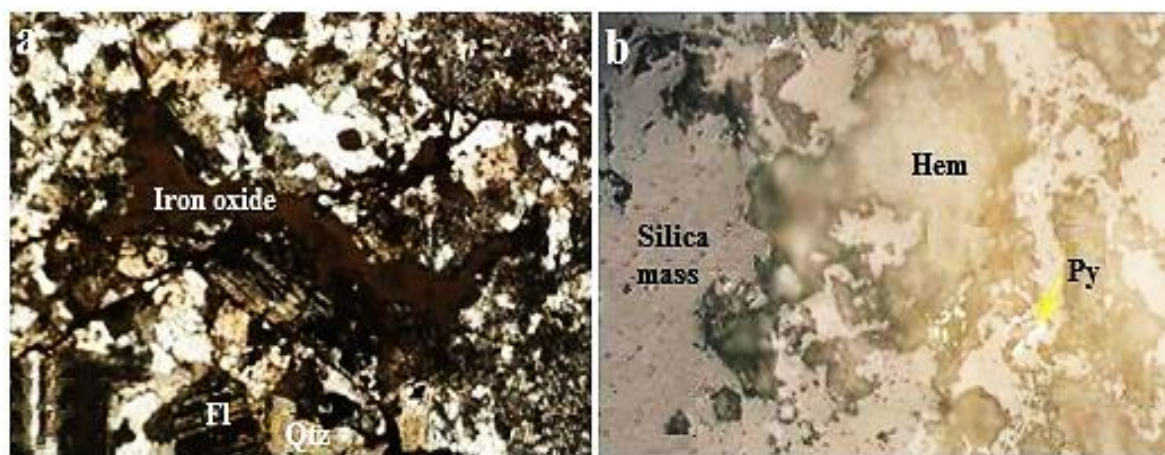


Figure 8 - Ore petrography and ore microscopy results for remotely-sensed altered samples in the Ramand region, (a) silica masses plus quartz and feldspars are common gangue minerals in gold-bearing samples, (b) the two main ores are hematite and pyrite



Fluid Inclusion Studies

Fluid inclusion microthermometry was carried out on inclusions in vein quartz using a Linkam THM600 heating-freezing stage fitted with a TMS-93 thermal control unit equipped with a Ziess microscope at the Iranian Mineral Processing Research Center (IMPRC) employing standard procedures (SHEPHERD *et al.*, 1985). The stages enable measurements within a temperature range of -196°C to $+600^{\circ}\text{C}$. Freezing and heating runs were undertaken using liquid nitrogen. The thermal resistor of the stage was calibrated by using standard natural and synthetic inclusions. Molar volumes, compositions and isochores were calculated with the help of FLINCOR (Brown, 1989). The salinity of aqueous fluid inclusions devoid of dissolved gases was calculated by the Bodnar's equation (BODNAR, 2003). Salinity from the final clathrate melting was calculated by the Diamond equation (1992). Fluid inclusion studies aimed to assess the nature and evolution of the mineralizing fluids as well as the physicochemical parameters controlling copper mineralization in the study area. According to abundance, nature and proportion of phases at room temperature, the studied fluid inclusions in the Ramand area were classified into three main types (Figure 10). Liquid-vapor (LV) inclusions consist of liquid and vapor. In this type of fluid inclusion, the liquid phase is volumetrically dominant and vapor bubbles constitute about 30% of the volume (Figure 11). The diameter of these fluid inclusions ranges from 8 to 20 μm . The other fluid inclusions are mono-phase vapor inclusions and liquid-rich two phase inclusions, both with limited abundance. Fluid inclusions were analyzed by cycles of freezing down to -196°C and heating up to $+600^{\circ}\text{C}$. The freezing-heating cycles were generally repeated several times to avoid nucleation-induced problems during freezing runs (Table 1). The initial (T_e) and final (T_m) ice melting temperatures of LV fluid inclusions were measured. The initial ice melting temperature of VL inclusions was difficult to determine because of the high vapor/liquid ratios. The first ice melting temperature (T_e) in most LV fluid inclusions was -21°C . This suggests the presence of NaCl and CaCl_2 as the main salts in the solution. The final melting temperature (T_m) for these inclusions ranges from -1.1 to -2.8°C corresponding to salinities of 1.75 to 4.74 wt % NaCl equivalent, respectively (Figure 12). The homogenization temperature of LV fluid inclusions ranges from 73 to 307°C .

Figure 9 - (a, b) Shiny appearances of gold particles (Au=gold, Ccp=chalcopyrite, scale bar = 10 μm)

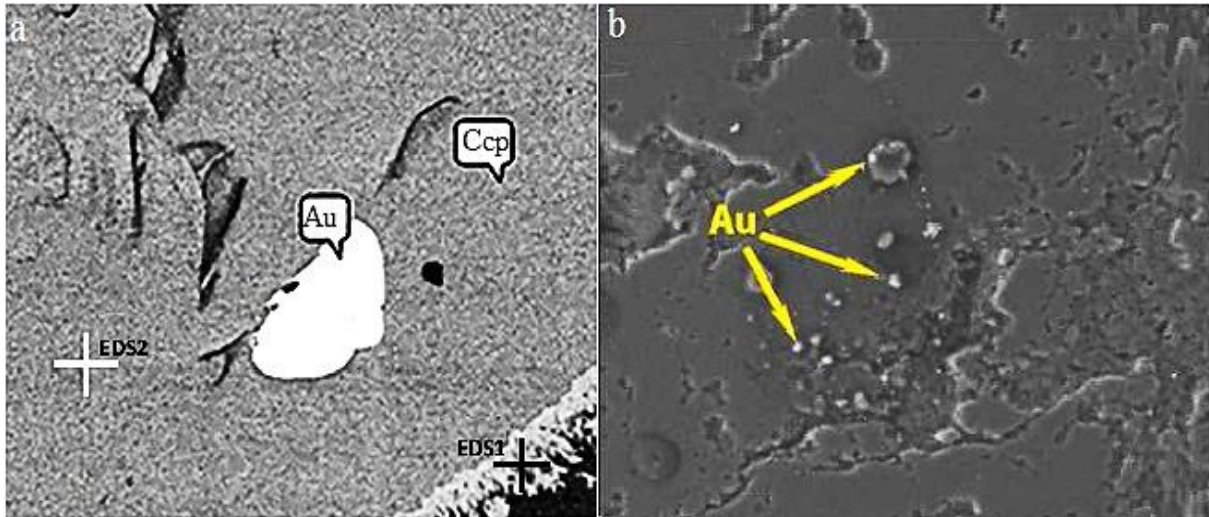


Figure 10 - Images of inclusions in rocks from Ramand area (scale bar = 30 μm) (a) Two-phase inclusions (L+V) consists of a gas phase (V) and liquid water (L) (800x magnification, from sample 5A), (b) two-phase inclusions rich in liquid (from sample 5A), (c) two-phase inclusions rich in liquid (from sample 5A) and (d) two-phase inclusions rich in liquid (from sample 5A).

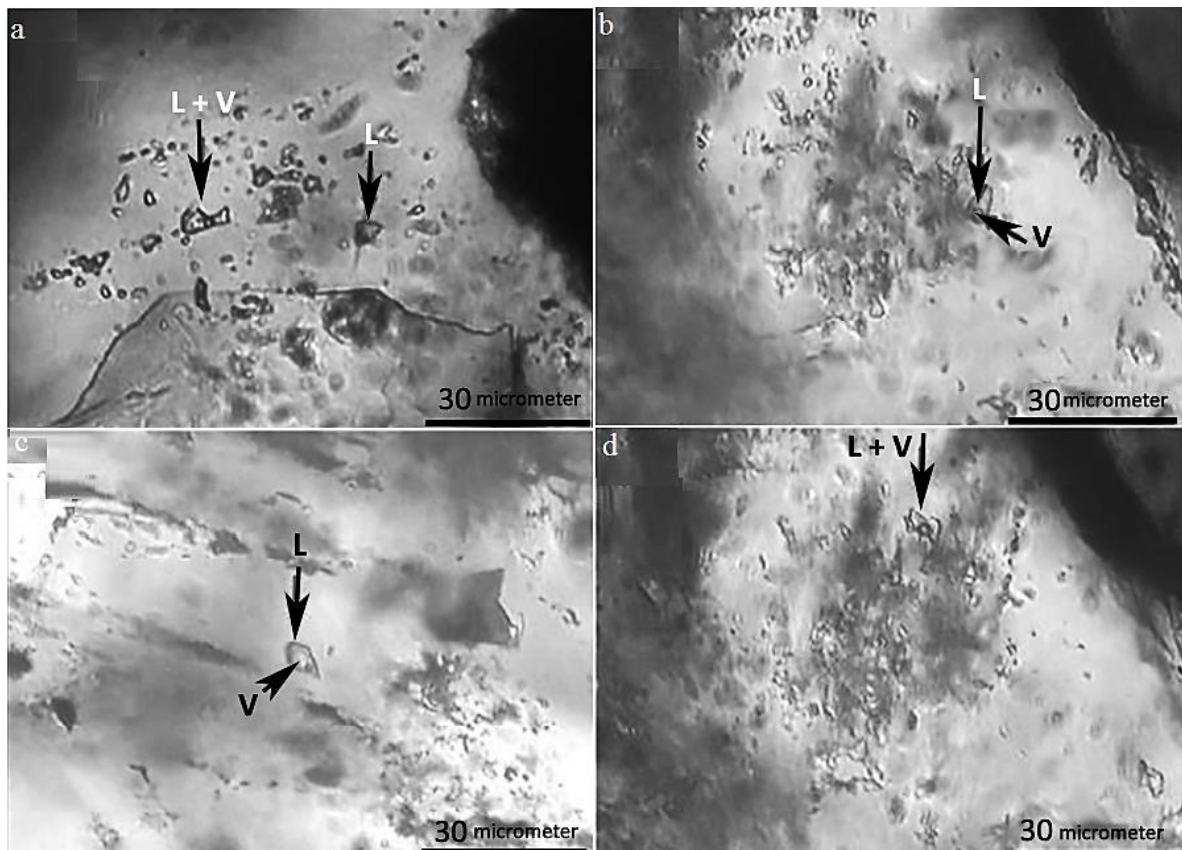
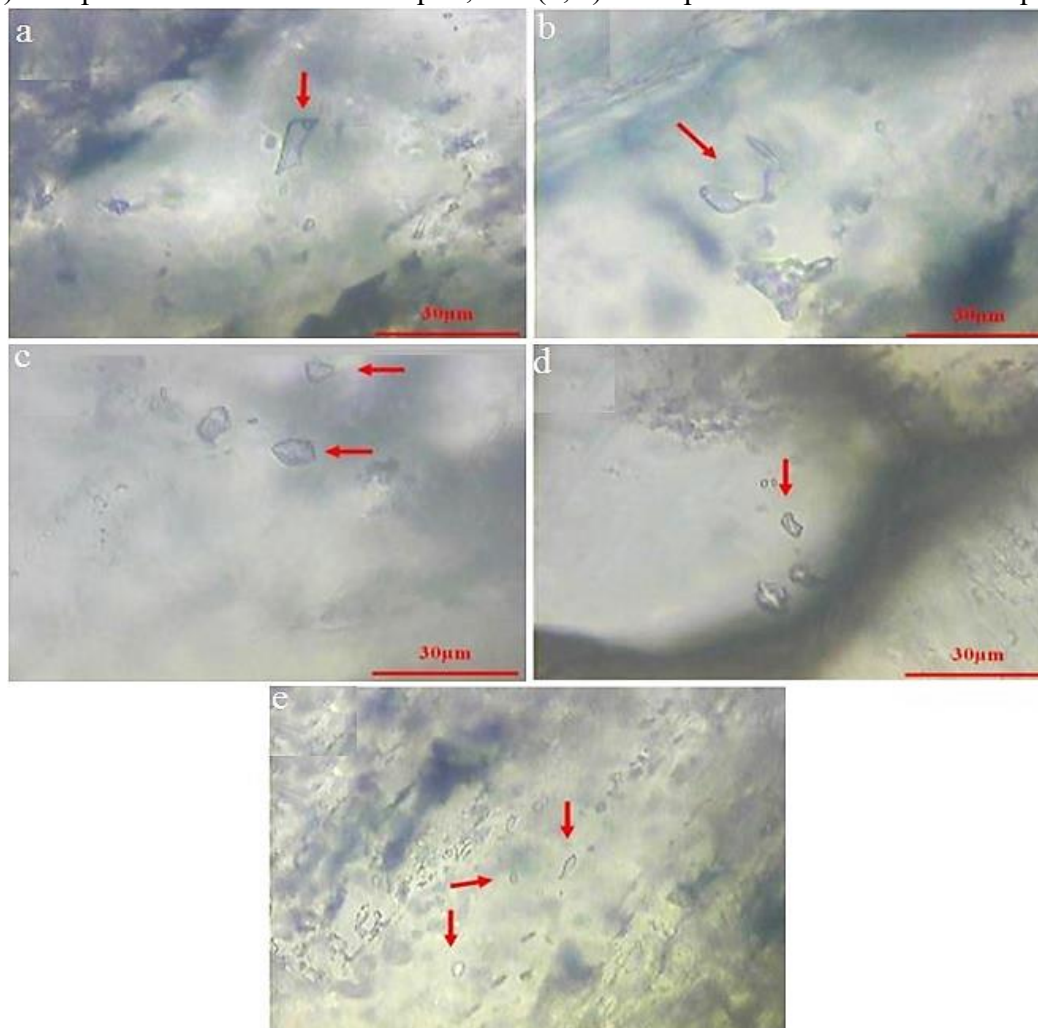


Figure 11 - Photomicrographs of fluid inclusions from mineralized quartz veins in the Ramand area, (a) two-phase LV inclusions (liquid + vapor), (b) necking-down phenomenon, (c) two-phase inclusions rich in liquid, and (d, e) monophasic inclusions rich in liquid.



Oxygen Isotopes

The $\delta^{18}\text{O}$ and δD values in a hydrothermal fluid may provide invaluable information on the origin of the fluid. However, the fluid's subsequent history must also be considered because of possible modification by isotopic exchange with enclosing rocks and minerals. In the Ramand area, oxygen isotope composition was studied in quartz and calcite from propylitic alteration zones. The $\delta^{18}\text{O}$ values in calcite vary from +4.4 to +9.4‰ with an average of +6.6‰. The $\delta^{18}\text{O}$ values in quartz range from 5.8 to 6.9‰ with an average of 6.5‰ (Table 2). There are at least two likely sources of water in the Ramand region for ore-forming fluids, namely magmatic water and local meteoric water.

Figure 12 - Histograms of homogenization temperatures and salinity of fluid inclusions in the Ramand area

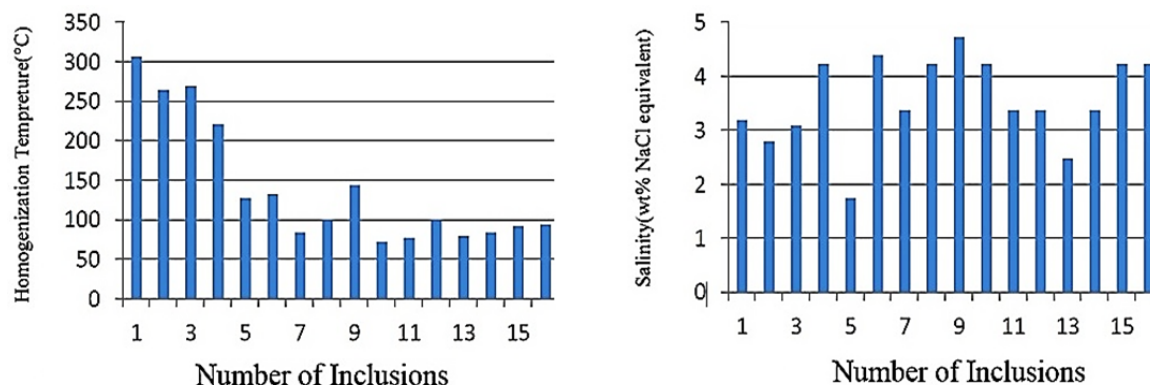


Table 1 - Results of Atomic Absorption Analysis (AA) for Au-bearing sample from Ramand

| Sample | M 28 | M 37 | M 31 | M 22 |
|----------|------|------|------|------|
| Au (ppb) | 131 | 133 | 125 | 145 |

Table 2 - Paragenetic sequence of ore and gangue minerals in the Ramand area.

| Minerals | Host Minerals | Hypogene Minerals | | Supergene Minerals |
|---|---------------|-------------------|---------|--------------------|
| | | Phase 1 | Phase 2 | |
| Calcite Dolomite Quartz | ===== | | ===== | |
| Pyrite Chalcopyrite Oligist Hematite | | ===== | ===== | |
| Chalcocite Covelite Goethite Limonite Malachite | | | | ===== |
| Veins-Veinlets Replacement Colloform | | ===== | ===== | ===== |

Results of Fluid Inclusion and Isotopic Studies

Studies on primary fluid inclusions and changes in oxygen isotopes in the Ramand mineralized samples indicate the dominance of pseudo-epithermal conditions with a dispersed

outcrop of gold veins (Au lode) (Table 3). These facies are associated with chalcopyrite and galena mineralogical sequences. Microscopic studies also indicate a paragenetic association between gold mineralization and the various sulfide compounds located in an area of siliceous minerals (especially quartz), clays, feldspar and calcite. The average gold value in the rich veins is 1000 mg/tonne with a maximum of 1750 mg/tonne. Rich veins with a favorable spatial location are observed with rhyodacite and trachyandesitic oligocene outcrops. The veins are most likely surrounded by a halo of silica, argillic, and propylitic alteration (with abundant chlorite and calcite). The structural stretching of the veins is in line with northwest-southeast faults and in some cases parallel to the east-west faults. Isotopic studies in the Ramand region validate that the hypogenic ore-bearing fluid often originated from magmatic fluids (based on the results in Table 3), as proven by the results of oxygen isotope studies on quartz and calcite minerals (Table 4). Table 5 lists the samples selected for isotopic analysis. In all three samples, the stable oxygen isotope content was utilized to determine the origin of minerals.

Table 3 - Fluid inclusion microthermometric data from Ramand area, Qazvin, Iran

| Sample | n | Size(µm) | Type | Origin | Temp (°C) | Tmice (°C) | wt% NaCl | Thv-l (°C) | Degree of Fill | Host Mineral |
|--------|---|----------|------|---------|-----------|------------|----------|------------|----------------|--------------|
| 5-A | 1 | 15 | L+V | Primary | nv | nv | 3.2 | 307 | 0.8 | Qtz |
| | 2 | 8 | | | | | 2.8 | 265 | | |
| | 3 | 8 | | | | | 4.24 | 270 | | |
| | 4 | 12 | | | -21 | -2.5 | 4.24 | 222 | | |
| | 5 | 12 | | | | -1.1 | 1.75 | 128 | | |
| | 6 | 15 | | | | -2.6 | 4.41 | 133 | | |
| | 7 | 12 | | | | -2 | 3.38 | 85 | | |
| | 8 | 15 | | | | -2.5 | 4.24 | 100 | | |
| 3-A | 1 | 20 | L+V | Primary | -21 | -2.8 | 4.74 | 145 | 0.9 | Qtz |
| | 2 | 18 | | | | -2.5 | 4.24 | 73 | | |
| | 3 | 20 | | | | -2 | 3.38 | 78 | | |
| | 4 | 15 | | | | -2 | 3.38 | 100 | | |
| | 5 | 10 | | | | -1.5 | 2.49 | 80 | | |
| | 6 | 15 | | | | -2 | 3.38 | 85 | | |
| | 7 | 17 | | | | -2.5 | 4.24 | 93 | | |
| | 8 | 20 | | | | -2.5 | 4.24 | 95 | | |

Table 4 - Oxygen isotope compositions of calcite and quartz from Ramand area, Qazvin, Iran

| Sample NO. | ¹⁸ O-Calcite (0/00) | ¹⁸ O-Quartz (0/00) | Qtz/Cc fractionation |
|------------|--------------------------------|-------------------------------|----------------------|
| 5A | 5.9 | 6.9 | 302.6 |
| 3A | 9.4 | 5.8 | 310.1 |
| 6B | 4.4 | 6.9 | 287.4 |

Table 5 - The samples selected for isotopic studies.

| Row | Number of specimens | Sampling location | | Gold content mg/tonne | Mineralogical background containing isotopes of oxygen | | |
|-----|---------------------|-------------------|------------|--------------------------|--|-----------------------------|------------------------------------|
| | | Longitude | Latitude | | Silicate | Carbonate-Sulfite | Oxide |
| 1 | 5A* | 49 44' 22" | 35 42' 32" | 820 | Quartz ,chlorite calcite | Pyrite | Not present |
| 2 | 3A* | 49 45' 30" | 35 42' 00" | 1250 | Quartz, chlorite, calcite | Pyrite | Goethite |
| 3 | 6B | 49 45' 03" | 35 42' 11" | 980 | Crystal quartz- glass | Pyrite and copper pyrite | Dispersed and micro hematite |

The results also indicate that atmospheric water was most likely mixed with the carbonate halo, rather than quartz veins. Consequently, the isotopic content of oxygen in the calcite collected from propylitic regions is less than that of quartz samples, leading to an increase in the probability of the mixing of atmospheric water with water in magmatic-hydrothermal systems in the Ramand region. Isotopic studies in this area indicate increased ^{18}O content in some samples. In this study, the changes in the ratio of oxygen isotopes ($^{16}\text{O}/^{18}\text{O}$) are in line with the Standard Mean Ocean Water standard (SMOW), indicating the relationship of silica alteration zone (quartz) with the Cenozoic magma infiltration process. In other words, magmatic-hydrothermal processes were responsible for silica alteration and formation of quartz, sericite, and pyrite facies, which is strongly in agreement with the results of micro-thermometric studies, indicating the role of hydrothermal systems (epithermal systems in particular). Overall, the microthermometric and isotopic investigation of samples from the area support the magmatic origin of the ores, although some mixture might have occurred between atmospheric and magmatic water. These findings suggest the importance of hydrothermal systems for the occurrence of alteration and mineralization phenomena. The relative abundance of isotope ^{18}O is a good indication of the origin of hydrothermal fluids. The conformity of location of the veins to the pattern of seam distribution and tectonic clefts indicates the influence of epigenetic phases on the mineralization process. Therefore, the results of both oxygen isotope analysis and initial fluid inclusion analysis propose a magmatic origin for the alteration phenomena which has been affected by tectonic factors during the final stages of the Cenozoic magmatic differentiation. It should be noted that the degree of salinity in mineralized fluids and homogenization temperature in microscopic samples correspond with the isotopic evidence and show the magmatic origin of the fluids and the occurrence of the boiling phase, in turn causing the development of alteration zones and mineralization in sericitic facies. The results of micro-thermometric studies revealed delayed subtraction of the magma in post-magmatic environments. This, in turn, results in the subtraction of the intermediate magma, an increase in ore-bearing fluids, and appearance of alteration halos around the mineral vein. According to the Wilkinson diagram

(2001), the location of Ramand samples within the Au-lode range indicates the probability of gold veins in this area. Furthermore, the genesis of fluid inclusions and the range of variations in their homogenization temperature (mainly liquid and vapor inclusions) are consistent with the mechanisms of epithermal systems. However, due to the lower salinity of the Ramand samples, the probability of detecting veins under pseudo-epithermal conditions is higher than an actual epithermal system (Figure 13). As can be seen, most inclusions are in mixing and dilution phases, indicating mixing of magmatic waters with each other and with atmospheric water. In the combination process of the diagram, orogenic fluids may be combined with those of a hypogenic origin. So, some inclusions have lower salinity while showing the same homogenization temperature (roughly 300 °C) (Figure 14). In contrast, the dilution of the fluid phases in other inclusions is associated with a significant decrease in the salinity of the ore-bearing fluid. These inclusions represent a dilution of fluids and validate the probability of mixture between magmatic water and atmospheric water. From a statistical point of view, after normalizing the distribution of inclusions, limited dilution is observed in sample 2, and most inclusions are in line with the process of composition. However, the inclusions of samples 1 and 3 pass both composition and dilution phases and are more likely to have been exposed to magmatic fluids and atmospheric water, compared to sample 2.

Figure 13 - The location of Ramand samples on the Wilkinson chart (2001). The variations in salinity and homogenization temperature are more proportional with the vein mineral resources

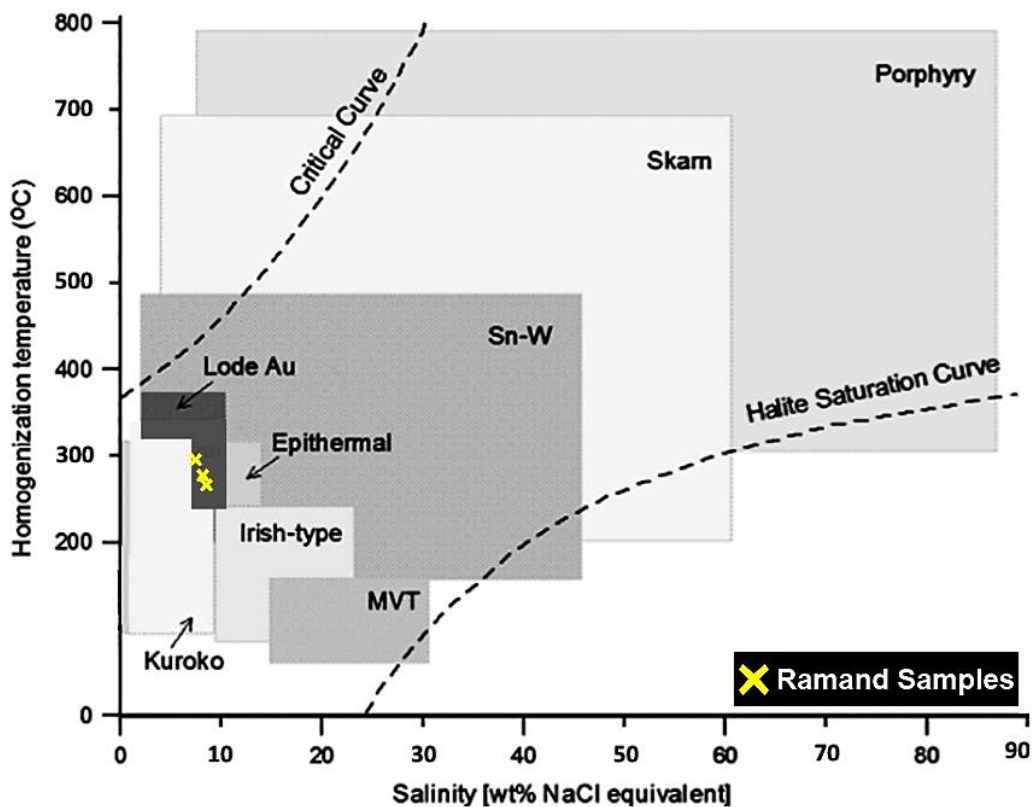
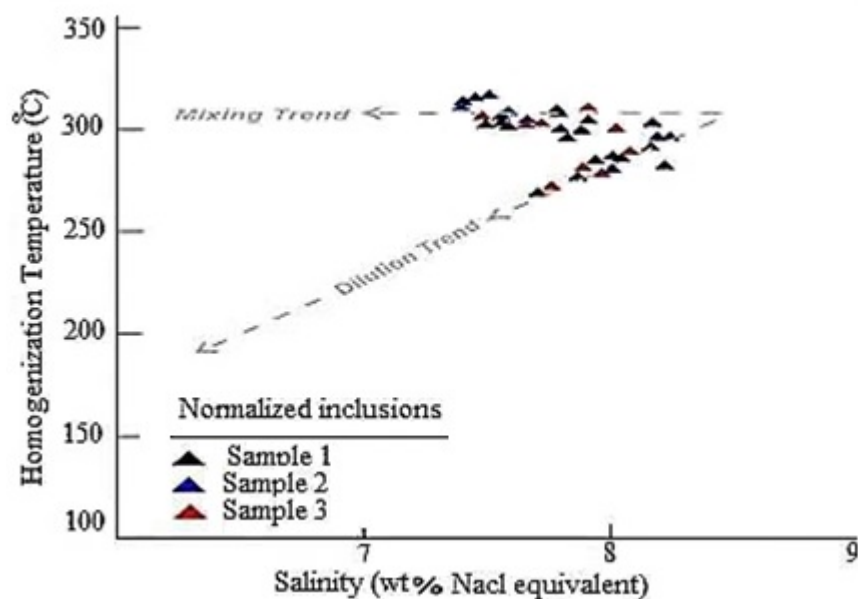


Figure 14 - By spot checking the inclusions and detailed study of changes in their salinity and homogenization temperature, the diagram was for samples 1 to 3



DISCUSSION

This study focused on extended altered regions and silica veins in Ramand region using field methods and micro-thermometry. An aggregated alteration containing clays and iron oxides was identified in the region. Sampling and results of instrumental analysis revealed the dominance of a clayey matrix within silica-based mineralization in this region. The prospected regions in Ramand area have adequate potential for epithermal mineralization because of a large number of solution-related alterations on the surface as well as evidence indicating continuous deep-underground alterations. Sulfide minerals and their textures may be interpreted to be primary contemporaneous with ore genesis, and their emplacements can be related to deep structural pathways for ore-fluid flow (BECHTEL *et al.*, 2001; BLUNDELL *et al.*, 2003; MUCHEZ *et al.*, 2005; McGOWAN *et al.*, 2006). Based on micro-thermometry in the study area, there are two sources of water for the ore-forming fluids, namely magmatic and meteoric water. The interaction between meteoric water and magmatic water caused a decrease in the magmatic fluid gradient, leading to a mixture of magmatic and meteoric fluid with a salinity of 1.75 to 4.74 wt % NaCl equivalent. This fluid caused alteration in parts of volcanic wall rocks and some argillic alteration. Late fractures or reopened veins provided pathways for this fluid to circulate in the system. The fluid's temperature increased during progressive circulation, causing destabilization of the previously formed K-feldspar and producing an alteration zone. This, in turn, led to leaching of previously formed copper sulfide minerals and precipitated a limited proportion of chalcopyrite in some parts of the phyllic alteration zone. Compared to other hydrothermal alteration types, phyllic alteration in the study area has developed only locally.

CONCLUSION

Based on petrography and mineralogy of vein and outcrop samples, silicic, phyllic, argillic and propylitic hydrothermal alterations were recognized in the Ramand region. Study

of thin sections confirmed the hydrothermal origin of ore-bearing solutions in a post-magmatic environment. Fluid inclusion studies showed the presence of two main hydrothermal fluids in the Ramand region. A mixture of magmatic fluid and meteoric water with moderate to high temperature and low salinity has been responsible for alterations in the volcanic wall rocks and copper mineralization. The $\delta^{18}\text{O}$ values of quartz and calcite in the Ramand region ranged from +4.4 to +9.4‰ suggesting a predominant magmatic origin for fluids in this index. The isotopic composition of oxygen suggests crystallization of quartz layers from magmatic-hydrothermal fluids. All these factors have made Ramand index a sub-economic ore deposit (ore-forming). Due to a large number of solution-related alterations on surfaces, this study area has potential for epithermal mineralization and paragenesis of post-magmatic mineralization in the altered regions, producing minerals such as kaolinite and jasperoid. This indicates continuous mineralization at the depths of the alteration zones. However, a deep investigation of altered features and corresponding mineralization processes is highly recommended for further exploration, with an emphasis on precious metal accumulations in the silica veins. The results of isotopic and micro-thermometric study of the fluid inclusions revealed the magmatic origin of sulfide minerals in the Ramand area, associated with differentiation processes and appearance of hydrothermal-epithermal systems. The subtraction index of oxygen isotopes in quartz and calcite in the three samples collected from Ramand mineralized regions was consistent with the isotopic criteria of the hypogenic regions. Based on fractionation Qtz/Cc boundary, mixing of surface water might be expected (a partial mixing is possible). The findings of micro-thermometry and salinity of fluid inclusions for the Ramand mineralized samples were in good agreement with oxygen isotope contents, representing a magmatic environment during subtraction. Due to proximity of the ore-bearing fluid to the boiling point, the two-phase liquid-vapor fluid has relatively increased. The nature of the fluid differs from that seen in porphyry systems. The mechanism of temperature homogenization is also more similar to hydrothermal-epithermal systems. The compatibility of samples with Wilkinson's chart show that the temperature ranges and salinity of the samples are similar to that of gold veins. With an increase in salinity, the samples are attributed to epithermal sources. Therefore, samples may be found at the depths of alteration facies with salinity and homogenization temperatures characteristic of epithermal environments. In summary, presence of iron, copper, lead, and gold mineralization (in the sulfide system) is of veins type and should be further evaluated and investigated using exploratory criteria.

REFERENCES

- AGHANABATI, A. **Geology of Iran**. Geological Survey of Iran, Tehran, Iran (in Persian), 2004.
- BAZARGANI-GUILANI, K., PARCHEKANI, M., NEKOUVAGHT TAK, M. Mineralization in the Taroum mountains, View to Barik-Ab Pb-Zn (Cu) deposit, Western Central Alborz, Iran, **WSEAS conferences**, Cambridge, London, 2008.
- BEANE, R., BODNAR, R. Hydrothermal fluids and hydrothermal alteration in porphyry copper deposits, **Arizona Geological Society Digest**, 1995.
- BECHTEL, A., SUN, Y., PÜTTMANN, W., HOERNES, S., HOEFS, J. Isotopic evidence for multi-stage base metal enrichment in the Kupferschiefer from the Sangerhausen Basin, Germany. **Chemical Geology**, 176: 31-49, 2001.
- BERBERIAN, F. **Petrogenesis of Iranian plutons: a study of the Natanz and Bazman**

intrusive complexes, University of Cambridge, Cambridge, 1981.

BERBERIAN, M., KING, G. Towards a paleogeography and tectonic evolution of Iran. **Canadian journal of earth sciences**, 18: 210-265, 1981.

BLUNDELL, D., KARNKOWSKI, P., ALDERTON, D., OSZCZEPALSKI, S., KUCHA, H. Copper mineralization of the Polish Kupferschiefer: a proposed basement fault-fracture system of fluid flow. **Economic Geology**, 98:1487-1495, 2003.

BODNAR, R. J. Introduction to aqueous-electrolyte fluid inclusions. Fluid inclusions. **Analysis and interpretation**, 32: 81-100, 2003.

BROWN, P. E. A microcomputer program for the reduction and investigation of fluid-inclusion data. **American Mineralogist**, 74:1390-1393, 1989.

COOKE, D.R., HOLLINGS, P., WALSH, J.L. Giant porphyry deposits: characteristics, distribution, and tectonic controls. **Economic geology**, 100: 801-818, 2005.

EZZATI, A., MEHRNIA, R., AJAYEBI, K. Detection of Hydrothermal potential zones using remote sensing satellite data in Ramand region, Qazvin Province, Iran. **Journal of Tethys**, 2: 93-100, 2014.

GUSTAFSON, L. B., HUNT, J. P. The porphyry copper deposit at El Salvador, Chile. **Economic Geology**, 70: 857-912, 1975.

MANSOURI, F. **Petrology of Eocene volcanic rocks in the southwest of Danesfehan area.** MSc Thesis, Tarbiat Moallem University of Tehran, Iran (in persian), 1998.

MCGOWAN, R.R., ROBERTS, S., BOYCE, A. J. Origin of the Nchanga copper–cobalt deposits of the Zambian Copperbelt. **Mineralium Deposita**, 40: 617-638, 2006.

MEHRNIA, S. R. Introducing the band M-ratio and its application in the diagnosis of hydrothermal alterations (case study: Ramand area in the southern province of Qazvin). **19 Congress of Iran Geology and 9th Geology National Conference of Payam Noor University**, Iran (in Persian), 2015.

MUCHEZ, P., HEIJLEN, W., BANKS, D., BLUNDELL, D., BONI, M., GRANDIA, F. Extensional tectonics and the timing and formation of basin-hosted deposits in Europe. **Ore Geology Reviews**, 27: 241-267, 2005.

NIAZI, M., ASUDEH, I., BALLARD, G., JACKSON, J., KING, G., MCKENZIE, D. The depth of seismicity in the Kermanshah region of the Zagros Mountains (Iran). **Earth and Planetary Science Letters**, 40:270-274, 1978.

SEEDORF, E. Porphyry deposits: Characteristics and origin of hypogene features. **Economic Geology**, 100: 251-298, 2005.

SHEPHERD, T.J., RANKIN, A.H., ALDERTON, D.H. A practical guide to fluid inclusion studies. **Blackie Academic & Professional**, New York, 1985.